NJC

ROYAL SOCIETY OF CHEMISTRY

PAPER

View Article Online
View Journal | View Issue

Cite this: *New J. Chem.*, 2023, **47**, 900

Fluorinated [2]rotaxanes with spirofluorene motifs: a non-symmetric distribution of the ring component along the axle component†

Showkat Rashid,[a] Takashi Murakami,[a] Hiroshi Koganezawa,[a] Yusuke Yoshigoe,[a] Shoichi Hosoya[b] and Shinichi Saito *[a]

Received 13th October 2022,
Accepted 27th November 2022

DOI: 10.1039/d2nj05021h

rsc.li/njc

Oxidative dimerization of terminal alkynes (Glaser coupling) triggered by spirofluorene derived macrocyclic phenanthroline–Cu complexes was implemented to synthesize a series of novel [2]rotaxanes. Size and structural variations among the components and their implications on the dynamic behaviour were investigated in detail through ^{1}H and ^{19}F NMR spectroscopy. Strong perturbations in the NMR spectra of the rotaxanes with substituted macrocyclic components with low symmetry indicated the non-symmetric distribution of the ring component along the axle component. In some [2]rotaxanes, localization of the ring component in the proximity of the 1,3-diyne moiety was observed.

Introduction

Mechanical entrapping of otherwise disparate constituents has played a quintessential role in broadening the canvas of modern supramolecular chemistry. This restricted positioning of dissimilar molecules eventually led to the development of mechanically interlocked molecules (MIMs) like rotaxanes, catenanes, knots, *etc.*[1,2] The potential applications of these MIMs in general and rotaxanes in particular in various fields like nanoelectronics, polymer chemistry, catalysis and medical science are continuously increasing their traction.[3–7] Accordingly, many synthetic methodologies like template synthesis, self-assembly, or metal mediated coupling reactions were developed to access these attractive targets through efficient ways.[8]

In addition to their alluring structural and physio-chemical attributes, control of the distribution of components in rotaxanes has been studied thoroughly to understand their dynamic behavior and elaborated further to develop stimuli-responsive molecular systems.[9] A localized distribution of the ring component along the axle has been achieved by introducing functional groups so that two components could interact (Fig. 1a).[1,2] Alternatively, introduction of a bulky substituent in the axle component that acts as a kinetic barrier resulted in the restricted movement of the ring component (Fig. 1b).[10] This restricted movement may have far reaching consequences on the properties and applications of these rotaxanes and represents an important area for further investigations.

We have been using resorcinol–stitched macrocyclic phenanthroline–Cu complexes for the synthesis of rotaxanes and catenanes by effectively harnessing the catalytic activity of these complexes.[11] We envisioned that the introduction of a substituted spiro structure with low symmetry into the ring component could also help to control the distribution of the ring component (Fig. 1c). In this article we report the synthesis of a series of novel spirofluorene-based [2]rotaxanes (Fig. 2).

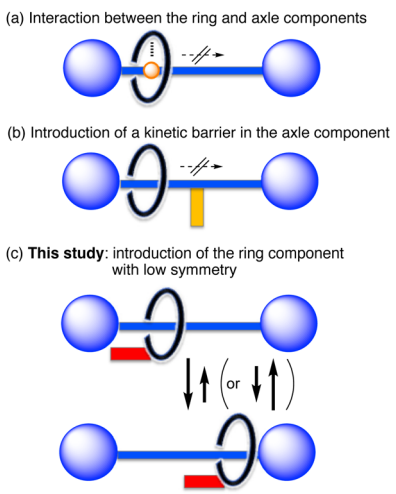

Fig. 1 Control of the distribution of the ring component in [2]rotaxanes.

[a] Department of Chemistry, Faculty of Science, Tokyo University of Science, 1–3 Kagurazaka, Shinjuku, Tokyo 162–8601, Japan. E-mail: ssaito@rs.tus.ac.jp
[b] Research Center for Medical and Dental Sciences, Tokyo Medical and Dental University, 1-5-45 Yushima, Bunkyo-ku, Tokyo 113-8510, Japan

† Electronic supplementary information (ESI) available: Experimental procedures, characterization, and copies of NMR spectra. See DOI: https://doi.org/10.1039/d2nj05021h

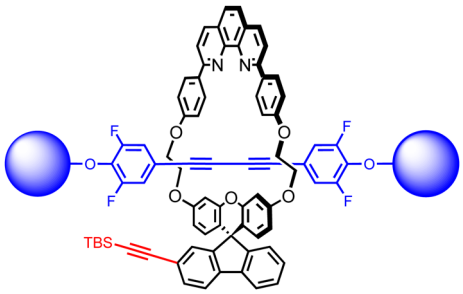

Fig. 2 [2]rotaxanes with a spirofluorene moiety.

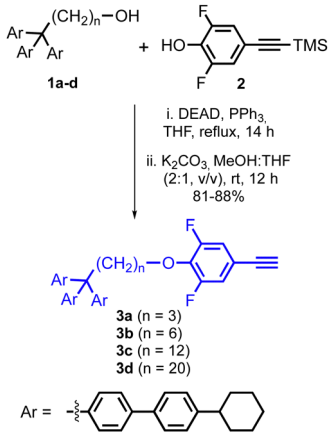

Scheme 1 Synthesis of axle precursors.

A non-symmetric distribution of the ring component was observed by introducing a spirofluorene motif with low symmetry into the ring component.

Our quest for the synthesis of spirofluorene based [2]rotaxanes commenced with the syntheses of fluorinated axle precursors (**3a–d**, Scheme 1). Fluorine atoms were introduced to utilize ^{19}F NMR spectroscopy for the conformational analysis of rotaxanes. Mitsunobu reaction was set up between alcohols (**1a–d**) bearing preinstalled terminal dumbbell moieties and TMS protected difluorophenol **2**. After the removal of the TMS group, the axle precursors (**3a–d**) with different alkyl chain lengths were isolated (Scheme 1).

With required axle precursors in hand, our next target was the design and synthesis of macrocyclic components based upon the spirofluorene motif. 2-iodospiro[fluorene-9,9′-xanthene]-3′,6′-diol **4A**, which acted as a common starting substrate, was synthesized from fluorene using a reported protocol.[12] Treatment of **4A** with various dibromides resulted in the formation of the corresponding dialkylated precursors **5A–D** in 73–94% yields (Table 1). To introduce bromoethyl groups, it was necessary to use an excess amount of 1,2-dibromoethane in the presence of K_2CO_3 and 18-crown-6 (entry 1).[13] The synthesis of other compounds proceeded under standard conditions devised for the alkylation of phenols (entries 2–4).[14]

The macrocyclic complexes **9A–D** were synthesized from **5A–D** in three steps (Scheme 2). Williamson's etherification of **5A–D** with **6**[15] produced the macrocycles **7A–D** bearing iodo

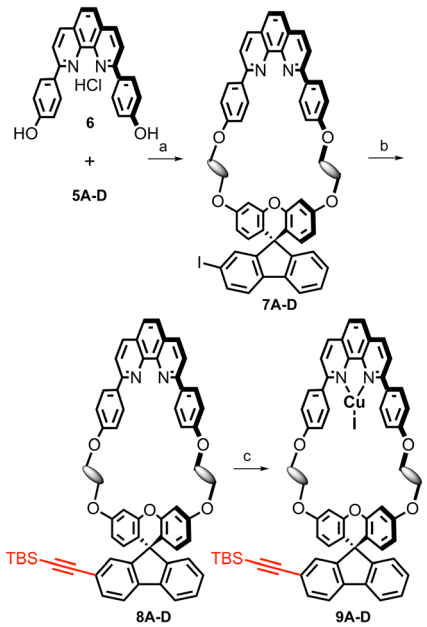

Scheme 2 Synthesis of macrocyclic phenanthroline–Cu complexes **9A–D**. Reagents and conditions, (a) K_2CO_3, DMSO : H_2O (99 : 1, v/v), 65 °C, 4 h, 59–68%; (b) $Pd(PPh_3)_4$, CuI, TBS acetylene, NEt_3 : DMF (dry, 1 : 2, v/v), rt, 18 h, 85–93%; (c) CuI, CH_2Cl_2 : CH_3CN (2.5 : 1, v/v), rt, 4 h, 90–95%.

Table 1 Synthesis of **5A–D** from **4A**

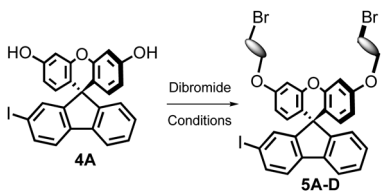

Entry	Dibromide	Cond.	Compd.		Yield (%)
1	$BrCH_2CH_2Br$ (excess)	K_2CO_3 18-crown-6 80 °C, 36 h	**5A**	CH_2CH_2	94
2	$BrCH_2CH_2CH_2Br$ (10 equiv.)	K_2CO_3 CH_3CN reflux, 4 h	**5B**	$CH_2CH_2CH_2$	73
3	$BrCH_2CH_2CH_2CH_2Br$ (10 equiv.)	K_2CO_3 CH_3CN reflux, 4 h	**5C**	$CH_2CH_2CH_2CH_2$	81
4	 (10 equiv)	K_2CO_3 CH_3CN reflux, 4 h	**5D**	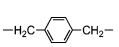	86

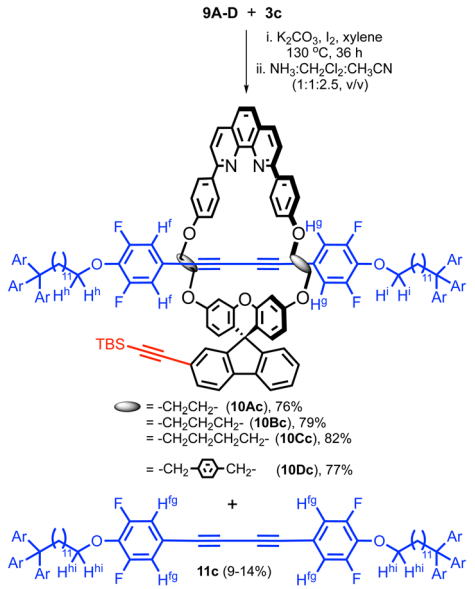

Scheme 3 Synthesis of rotaxanes with different macrocycles.

functionality. Sonogashira reaction of **7A–D** with (*tert*-butyldimethylsilyl)acetylene (TBS acetylene) gave the macrocycles **8A–D** with a spiro structure. Reaction of **8A–D** with CuI produced the spirofluorene based macrocyclic copper complexes **9A–D**.

Copper complexes **9A–D** and the axle precursor **3c** having a 12 carbon alkylene chain were used for the synthesis of rotaxanes incorporating different sizes of macrocyclic components (Scheme 3). A mixture of **9A–D** (1 equiv.), terminal alkyne **3c** (2.5 equiv.), I_2 (1.3 equiv.), and K_2CO_3 (3.8 equiv.) in dry xylene was heated at 130 °C for 24–36 h in a sealed tube. The oxidative dimerization of the terminal alkyne proceeded and metal complexed rotaxanes were formed. Demetallation was carried out by the addition of aqueous ammonia[16] to yield rotaxanes **10Ac–10Dc** along with the dimerized axle component **11c** as a minor product. The influence of the structure of macrocycle on the yields of rotaxanes (76–82%) was small.

The ^{1}H NMR spectrum of the rotaxane **10Ac** was recorded in $CDCl_3$[17] and the spectrum was compared with those of the corresponding axle (**11c**) and ring (**8A**) components (Fig. 3). A notable difference between the spectra of the rotaxane **10Ac** and axle component **11c** is the splitting of some signals. In the spectrum of **11c**, a doublet integrating to 4 protons was observed at 7.03 ppm and this signal was assigned to H^{fg} (Scheme 3). In the spectrum of rotaxane, splitting of this signal was observed and the two signals corresponding to H^f and H^g appeared at 6.68 and 7.50 ppm, respectively (Fig. 3).[18] A similar splitting pattern was observed in the 3.7–4.2 ppm region. A triplet was observed at 4.15 ppm in the spectrum of the axle component **11c** which was assigned as H^{hi} (Scheme 3). This signal appeared as two separate signals (H^h and H^i) in the NMR spectrum of rotaxane **10Ac** which were observed at 4.03 and 3.83 ppm, repectively (Fig. 3). This large separation was induced by the presence of the ring component with a less symmetric spiro structure. The signals of the ring component

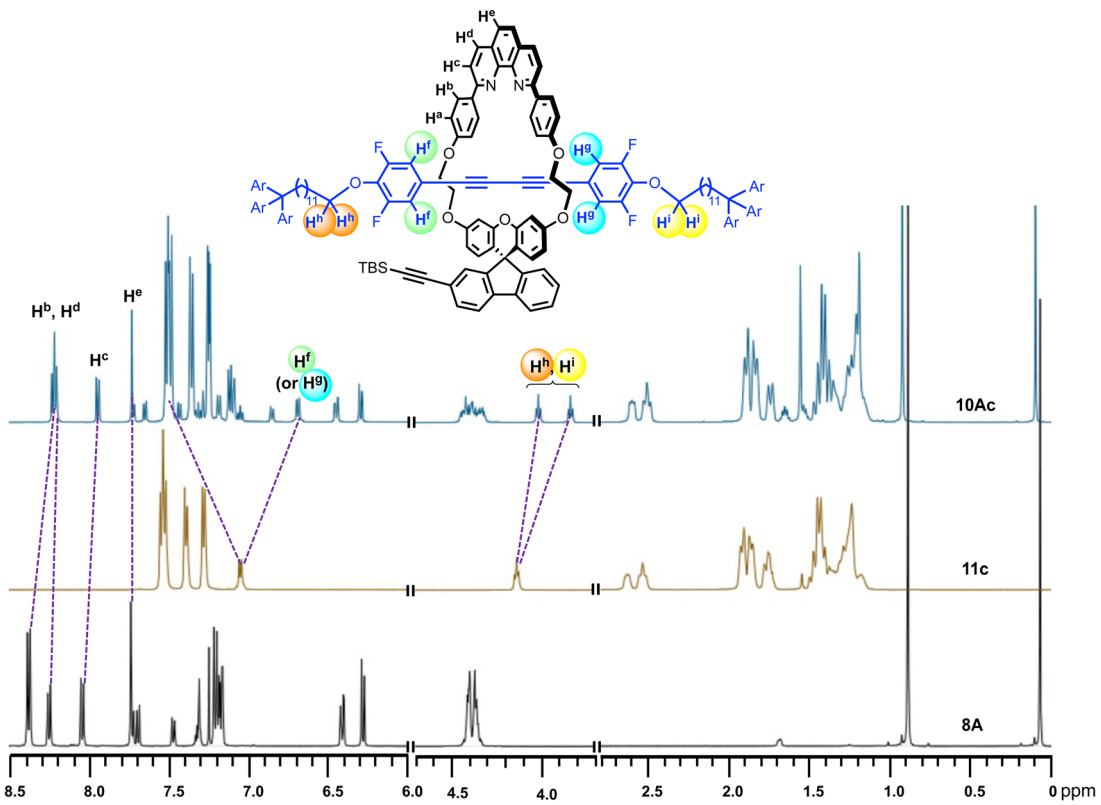

Fig. 3 Comparison of ^{1}H NMR spectra of rotaxane **10Ac**, axle component **11c** and ring component **8A** ($CDCl_3$, 500 MHz).

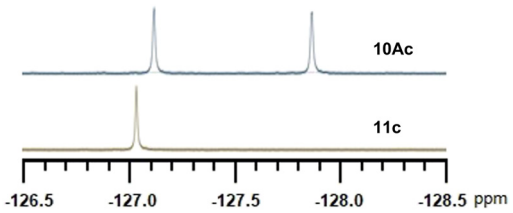

Fig. 4 ^{19}F NMR spectra of rotaxane **10Ac** and axle component **11c** ($CDCl_3$, 377 MHz).

8A above 7.5 ppm showed a slight upfield shift in rotaxane **10Ac**. For instance, the two doublets at 8.37 and 8.24 ppm in **8A** shifted to 8.20 ppm in **10Ac**. This small upfield shift was frequently observed in other rotaxanes we synthesized.

To gain further insights, ^{19}F NMR spectra of the rotaxane **10Ac** and the axle component **11c** were compared (Fig. 4). Two separate signals for the fluorine atoms on the two aromatic rings of **10Ac** were observed at −127.1 and −127.9 ppm, while a signal at −127.0 ppm was observed for **11c**. The emergence of these two distinct signals reconfirmed the loss of symmetry of the system.

Encouraged by these findings, a comparative study of ^{1}H NMR spectra of rotaxanes **10Ac–10Dc** was carried out and the reduced symmetry of the axle component in the rotaxanes was reflected in the NMR spectra, although to different extent (Fig. 5). In the ^{1}H NMR spectra, overlapping of the signals was observed in **10Cc** and the analysis of the data was difficult (Fig. 5a). In other rotaxanes, a clear tendency was observed: the

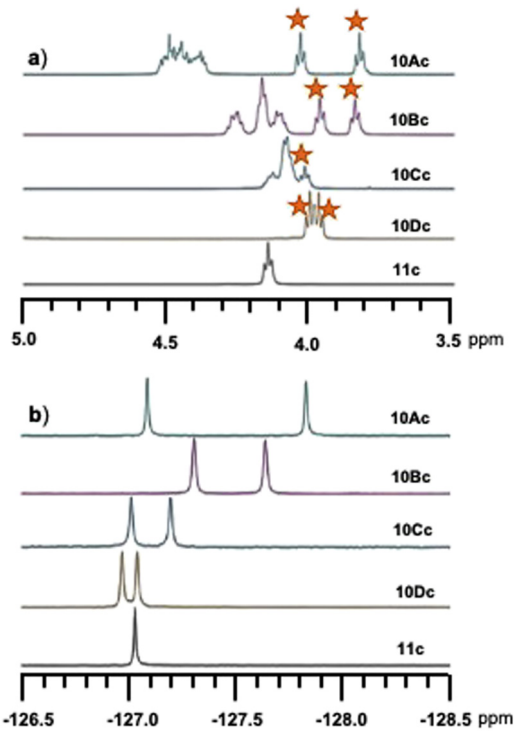

Fig. 5 Comparison of (a) ^{1}H and (b) ^{19}F NMR spectra of rotaxanes **10Ac–10Dc** and the axle component **11c** ($CDCl_3$, 500 MHz for ^{1}H and 377 MHz for ^{19}F). The signals of H^h and H^i (Fig. 3) are marked with an asterisk.

Table 2 ^{19}F NMR chemical shifts (ppm, $CDCl_3$, 377 MHz) of the rotaxanes **10Ac–10Dc** and the axle component **11c**

Entry	Linker	Compound	δF		$\Delta\delta F^a$
1	-CH$_2$CH$_2$-	**10Ac**	−127.12	−127.87	0.75
2	-CH$_2$CH$_2$CH$_2$-	**10Bc**	−127.31	−127.65	0.34
3	-CH$_2$CH$_2$CH$_2$CH$_2$-	**10Cc**	−127.00	−127.18	0.18
4	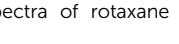	**10Dc**	−126.98	−127.05	0.07
5	(Axle component)	**11c**	−127.03		—

^{a} $\Delta\delta F$ = δF (low field) − δF (high field).

emergence of two separate signals and an upfield shift of one of the methylene groups was encountered in the spectra of rotaxanes **10Ac** and **10Bc**. Although we expected that the introduction of an aromatic ring in the linker would influence the chemical shifts of the methylene group, the observed difference in the chemical shifts was smallest for **10Dc,** which can be attributed to the increased size of the macrocycle.

As compared to the ^{1}H NMR spectra, the ^{19}F NMR spectra could be analyzed with ease. The overlap of the signals did not occur, and two well separated signals were observed in rotaxanes **10Ac–10Dc** (Fig. 5b). The observed values for ^{19}F signals are summarized in Table 2. These signals mostly appeared between −127 to −128 ppm and a maximum difference of 0.75 ppm was observed between the two signals in case of **10Ac**. As expected, the difference in the chemical shifts between two ^{19}F signals decreased (from 0.75 ppm in the case of **10Ac** to 0.07 ppm in the case of **10Dc**) as the size of the ring component increased.

Based on the observed upfield shifts of the signals of the methylene groups in the ^{1}H NMR spectra (Fig. 5a) and the fluorine signals in the ^{19}F NMR spectra (Fig. 5b) of **10Ac–10Dc** compared to those of the corresponding axle component **11c**, we assumed that the upfield shifts were induced by the presence of the ring component in the proximity of the axle component. The splitting of the signals of the axle component in rotaxanes **10Ac–10Dc** could be explained in two ways (Fig. 6). A simple ''substituent effect'' may be responsible for the observed spectra. The distribution of the ring component along the axle moiety would not be significantly affected by the spiro structure with low symmetry and the difference in the substituents attached to the spiro moiety (alkynyl group vs hydrogen atom) induced the difference in the observed chemical shifts (Fig. 6a). Alternatively, the distribution of the ring component could be modulated by the low symmetry of the spiro moiety (Fig. 6b). The presence of the bulky alkynyl group might induce a non-symmetric distribution of the ring component along the axle component, and a difference in the chemical shifts would be observed.

To understand the observed chemical shifts in the NMR spectra in depth, we synthesized symmetric spirofluorene based rotaxanes and observed their NMR spectra. Once again, the synthesis commenced from spirofluorene based diols **4B** and **4C**, readily accessible from a reaction of parent fluorenone

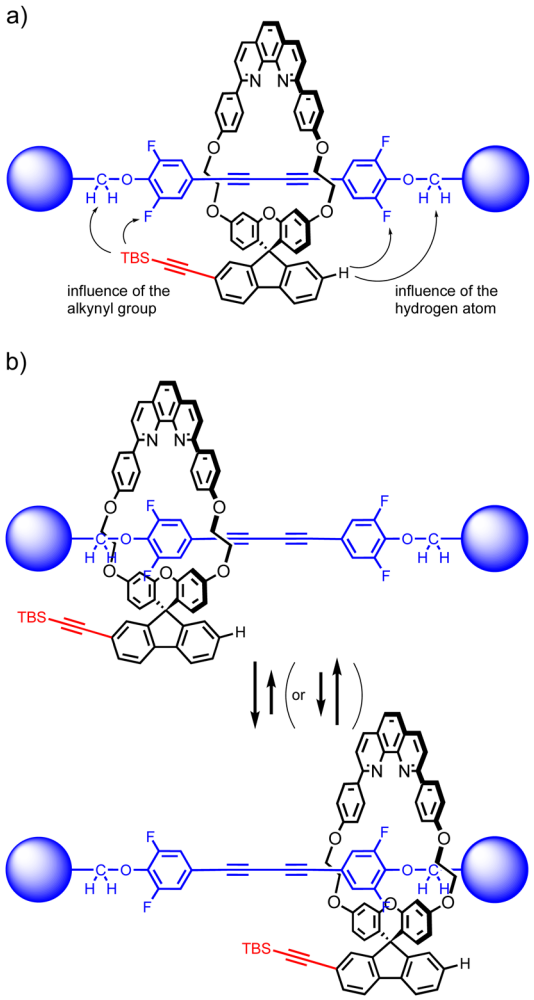

Fig. 6 Possible explanations for the difference in the NMR chemical shifts of **10Ac**. (a) "Substituent effect": the influence of (different) substituents on the ^{1}H and ^{19}F NMR chemical shifts of the rotaxanes. (b) Difference in the distribution of the ring component induced by the presence of different substituents.

or diiodofluorenone with resorcinol (Scheme 4).[13] Compounds **4B** and **4C** upon dialkylation furnished **12** and **13**. Solubility issues associated with **4C** prompted us to slightly change the reaction sequence and a sequential dialkylation followed by a Sonogashira reaction was implemented (to install the two silylacetylene functionalities) prior to Williamson's etherification to yield **13**. Williamson's etherification of **12** and **13** with **6** resulted in the formation of macrocyclic complexes **14** and **15**. Treatment of these macrocycles with CuI produced the copper complexes **16** and **17**.

With symmetrical macrocyclic copper complexes at our disposal, we synthesized corresponding rotaxanes using **3c** as the axle precursor (Scheme 5). Oxidative dimerization was facilitated between the macrocyclic copper complexes (**16** and **17**) and the axle precursor **3c**. The reaction of **16** was performed in THF at 75 °C and the rotaxane **18** was isolated in 66% yield. The reaction of **17** was performed in xylene at 130 °C and the yield of rotaxane **19** was 74%.

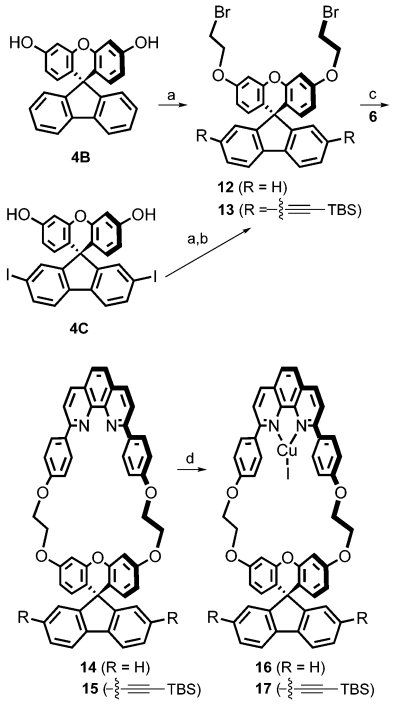

Scheme 4 Synthesis of macrocyclic phenanthroline–Cu complexes with a symmetric spirofluorene moiety. *Reagents and conditions*, (a) K_2CO_3, 18-crown-6, $BrCH_2CH_2Br$, 80 °C, 36 h, 91% (for **12** from **4B**); (b) $Pd(PPh_3)_4$, CuI, TBS acetylene, NEt_3 : DMF (dry, 1 : 2, v/v), rt, 18 h, 76% (for **13**, over two steps from **4C**); (c) **6**, K_2CO_3, DMSO : H_2O (99 : 1, v/v), 65 °C, 4 h, 59–68%; (d) CuI, CH_2Cl_2 : CH_3CN (2.5 : 1, v/v), rt, 4 h, 89–92%.

The ^{1}H and ^{19}F NMR spectra of **18** and **19** were compared with those of diyne **11c** (Fig. 7). As expected, the symmetric nature of **18** and **19** was reflected in the NMR spectra, and only

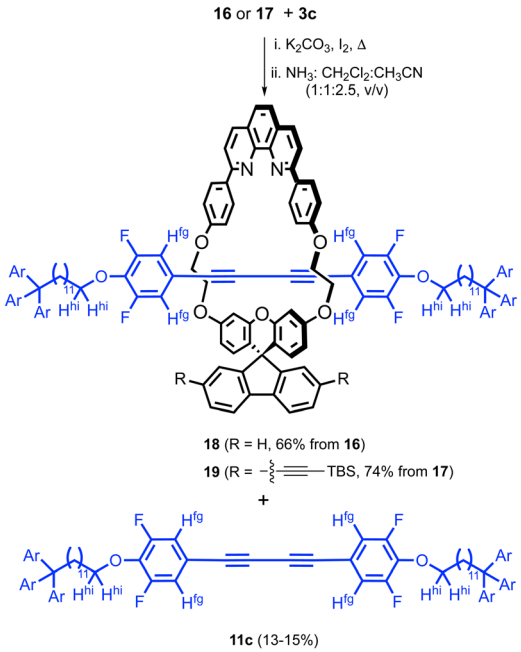

Scheme 5 Synthesis of rotaxanes with high symmetry.

one signal was observed for the two-methylene proton sets as well as fluorine atoms on the axle component. High-field shifts were observed for H^{hi} (Scheme 5) in **18** and **19**, and the difference in chemical shifts between the methylene protons (H^{hi}, Scheme 5) of **18** and **19** was very small (Fig. 7a). Similar results were observed in the ^{19}F NMR spectra; the observed chemical shift was influenced by the presence of the ring component, but it was not essentially influenced by the presence (or the absence) of an alkynyl group in the ring component (Fig. 7b). The results strongly imply that a simple "substituent effect" (Fig. 6a) is not operating in the rotaxanes, since the observed difference in the spectra between **18** and **19** was very small. Therefore, the observed splitting of the signals in the NMR spectra of **10Ac** should have been induced by a non-symmetric distribution of the ring component along the axle component (Fig. 6b).

The distribution of the ring component along the axle component in rotaxanes was further studied by comparing the NMR spectra of rotaxanes with different axle lengths. We assumed that the distribution of the ring component would be affected by the length of the axle if the ring component was not preferentially located at a specific position. The influence of the ring component would be more pronounced in rotaxanes with a shorter axle since the probability of its presence at a specific position on the axle component would increase. Accordingly, a larger effect of the ring component on the chemical shifts of the axle component could be observed in rotaxanes with a shorter axle component. To confirm this, macrocycle **9A** and axle precursors with different alkylene chain lengths (**3a,b,d**) were used to synthesize the rotaxanes with various axle lengths (Scheme 6). Reaction of **3a,b,d** with **9A** gave rotaxanes **10Aa**, **10Ab** and **10Ad** along with the dimers of the alkynes. The yields of **10Ab** (73%) and **10Ad** (78%) were satisfactory while the yield

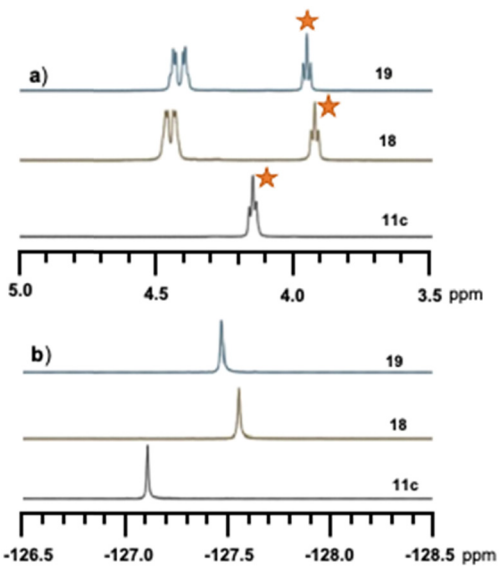

Fig. 7 Comparison of (a) ^{1}H and (b) ^{19}F NMR spectra of rotaxanes with symmetrical macrocycles ($CDCl_3$, 500 MHz for ^{1}H and 377 MHz for ^{19}F). The signals of H^{hi} (Scheme 5) are marked with an asterisk.

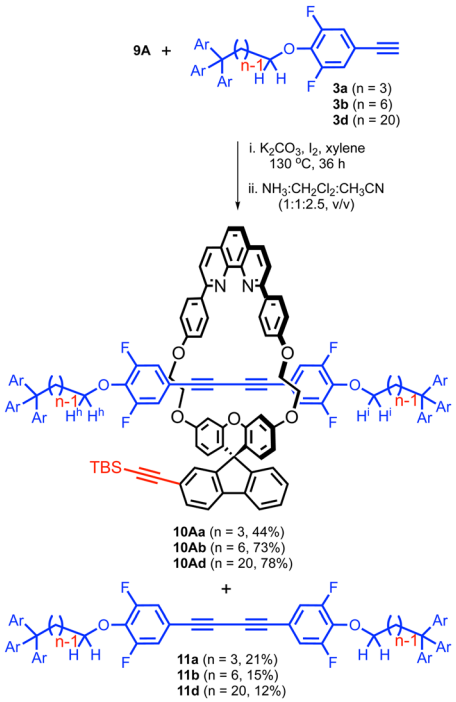

Scheme 6 Synthesis of rotaxanes with different axle lengths.

of **10Aa** was low (44%). The decreased yield of **10Aa** can be attributed to the increased steric bulk of the alkyne **3a,** which slowed down the threading reaction. Although the reactive ethynyl moiety in **3a** is far from the bulky triarylmethyl group, the presence of a vertically oriented TBS ethynyl group in **9A** would retard the formation of the alkynylcopper intermediate.

The ^{1}H and ^{19}F NMR spectra of **10Aa–10Ad** were recorded and the results are summarized in Fig. 8. Unexpectedly, the chemical shifts of H^{h} and H^{i} (Scheme 6) remained almost constant in the ^{1}H NMR spectra (Fig. 8a). Similarly, in the ^{19}F NMR spectra we did not encounter any large differences in the chemical shifts and the difference between the two signals was mostly around 0.7 ppm (Fig. 8b).[19] We initially anticipated that the distribution of the ring component in rotaxanes should be described as shown in Fig. 9a. The ring component of **10Ac**, for example, would be distributed throughout the axle component except for the bulky dumbbell moieties, and a non-symmetric distribution would be induced by the presence of a less symmetric spiro moiety. In this case, high-field shifts of the signals of the methylene groups as well as the fluorine atoms would be observed as the length of the axle component becomes short. This assumption is based on the result that the high-field shifts of the signals were observed when the signals of the rotaxane were compared with those of the axle component and on the postulation that the probability of the presence of the ring component at a specific position would increase in shorter rotaxanes such as **10Aa** (Fig. 9a). The observed results, however, could not be explained by the abovementioned assumption, because the chemical shifts were hardly influenced by the length of the axle component (Fig. 8). Instead, the results strongly indicate that there is localization of the macrocycle

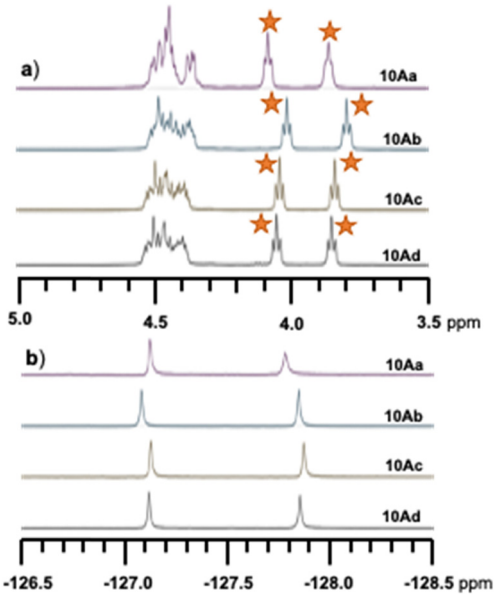

Fig. 8 Comparison of (a) ^{1}H and (b) ^{19}F NMR spectra of rotaxanes with various axle lengths ($CDCl_3$, 500 MHz for ^{1}H and 377 MHz for ^{19}F). The signals of H^h and H^i (Schemes 3 and 6) are marked with an asterisk.

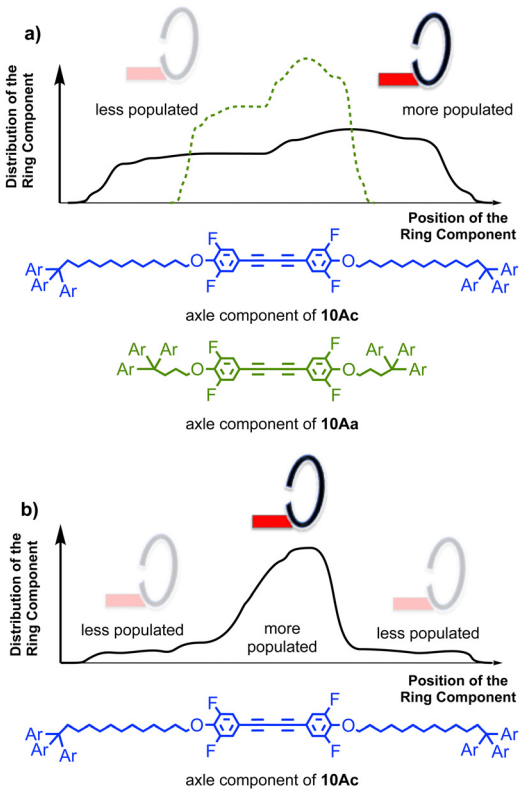

Fig. 9 (a) Initially anticipated distribution (solid line for **10Ac** and dashed line for **10Aa**) of the ring component in rotaxanes. (b) Revised distribution of the ring component in rotaxane **10Ac**. A localized, non-symmetric distribution was observed.

near the diyne functionality, and the ring component is less distributed along the alkylene moiety (Fig. 9b).[20] The difference

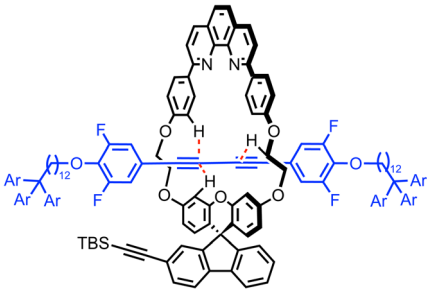

Fig. 10 Possible weak interactions which induced the localization of the ring component in **10Ac**.

in the distribution in a limited area (diyne moiety) would be responsible for the observed difference in the chemical shifts.[21] The observed result contrasts with our previous studies on rotaxanes with larger ring components.[9] The localized distribution can be explained in terms of the possible weak C–H...π interactions between the diyne functionality and the ring component (Fig. 10). This type of interaction has been reported in the solid state by several groups including ours.[22] The bulkiness of the alkylene chain compared to the diyne structure could also be a driving force for the localization of the ring component in the proximity of the diyne moiety.

Conclusions

In conclusion, we have outlined a general synthetic strategy, amenable to diversity creation for assembling spirofluorene based novel [2]rotaxanes in a high yielding and efficient manner. Detailed analyses of the ^{19}F and ^{1}H NMR spectra revealed that the distribution of the ring component in rotaxanes could be modulated by the introduction of a less symmetric spiro moiety into the ring component. Localization of the cyclic component in the proximity of the 1,3-diyne moiety was observed. This study would contribute to the understanding of the relationship between the structure and conformation of the rotaxanes.

Conflicts of interest

There are no conflicts to declare.

Acknowledgements

This work was supported by JSPS KAKENHI (grant number JP19K05442 and JP22K03071) and The Science Research Promotion Fund provided by The Promotion and Mutual Aid Corporation for Private Schools of Japan.

Notes and references

1 For selected reviews on interlocked compounds, see: (*a*) C. Dietrich-Buchecker and J. P. Sauvage, Interlocking

of molecular threads: from the statistical approach to the templated synthesis of catenands, *Chem. Rev.*, 1987, **87**, 795–810; (*b*) J.-P. Sauvage, Interlacing molecular threads on transition metals: catenands, catenates, and knots, *Acc. Chem. Res.*, 1990, **23**, 319–327; (*c*) D. B. Amabilino and J. F. Stoddart, Interlocked and Intertwined Structures and Superstructures, *Chem. Rev.*, 1995, **95**, 2725–2828; (*d*) R. Jager and F. Vögtle, A New Synthetic Strategy towards Molecules with Mechanical Bonds: Nonionic Template Synthesis of Amide-Linked Catenanes and Rotaxanes, *Angew. Chem., Int. Ed. Engl.*, 1997, **36**, 930–944; (*e*) S. A. Nepogodiev and J. F. Stoddart, Cyclodextrin-Based Catenanes and Rotaxanes, *Chem. Rev.*, 1998, **98**, 1959–1976; (*f*) J. E. Beves, B. A. Blight, C. J. Campbell, D. A. Leigh and R. T. McBurney, Strategies and Tactics for the Metal-Directed Synthesis of Rotaxanes, Knots, Catenanes, and Higher Order Links, *Angew. Chem., Int. Ed.*, 2011, **50**, 9260–9327; (*g*) E. A. Neal and S. M. Goldup, Chemical consequences of mechanical bonding in catenanes and rotaxanes: isomerism, modification, catalysis and molecular machines for synthesis, *Chem. Commun.*, 2014, **50**, 5128–5142; (*h*) M. Xue, Y. Yang, X. Chi, X. Yan and F. Huang, Development of Pseudorotaxanes and Rotaxanes: From Synthesis to Stimuli-Responsive Motions to Applications, *Chem. Rev.*, 2015, **115**, 7398–7501; (*i*) J. E. M. Lewis, M. Galli and S. M. Goldup, Properties and emerging applications of mechanically interlocked ligands, *Chem. Commun.*, 2017, **53**, 298–312; (*j*) F. Niess, V. Duplan and J.-P. Sauvage, Molecular Muscles: From Species in Solution to Materials and Devices, *Chem. Lett.*, 2014, **43**, 964–974; (*k*) M. Denis and S. M. Goldup, The active template approach to interlocked molecules, *Nat. Rev. Chem.*, 2017, **01**, 0061; (*l*) P. R. McGonigal, Multiply threaded rotaxanes, *Supramol. Chem.*, 2018, **30**, 782–794; (*m*) H.-Y. Zhou, Q.-S. Zong, Y. Han and C.-F. Chen, Recent advances in higher order rotaxane architectures, *Chem. Commun.*, 2020, **56**, 9916–9936; (*n*) A. de Juan, D. Lozano, A. W. Heard, M. A. Jinks, J. M. Suarez, G. J. Tizzard and S. M. Goldup, A chiral interlocking auxiliary strategy for the synthesis of mechanically planar chiral rotaxanes, *Nat. Chem.*, 2022, **14**, 179–187; (*o*) S. Rashid, Y. Yoshigoe and S. Saito, Phenanthroline based rotaxanes: recent developments in syntheses and applications, *RSC Adv.*, 2022, **12**, 11318–11344.

2 For selected books on interlocked compounds, see: (*a*) G. Schill, *Catenanes, Rotaxanes and Knots*, Academic Press, New York, 1971; (*b*) *Molecular Catenanes, Rotaxanes and Knots*, ed. J. P. Sauvage, C. Dietrich-Buchecker, Wiley-VCH, New York, 1999; (*c*) C. J. Bruns and J. F. Stoddart, *The Nature of the Mechanical Bond: From Molecules to Machines*, John Wiley & Sons, 2016.

3 (*a*) C. P. Collier, G. Mattersteig, E. W. Wong, Y. Luo, K. Beverly, J. Sampaio, F. M. Raymo, J. F. Stoddart and J. R. Heath, A [2]Catenane-Based Solid State Electronically Reconfigurable Switch, *Science*, 2000, **289**, 1172–1175; (*b*) H. Yu, Y. Luo, K. Beverly, J. F. Stoddart, H.-R. Tseng and J. R. Heath, The Molecule–Electrode Interface in Single-Molecule Transistors, *Angew. Chem., Int. Ed.*, 2003, **42**, 5706–5711; (*c*) J. W. Choi, A. H. Flood, D. W. Steuerman, S. Nygaard, A. B. Braunschweig, N. N. P. Moonen, B. W. Laursen, Y. Luo, E. DeIonno, A. J. Peters, J. O. Jeppesen, K. Xu, J. F. Stoddart and J. R. Heath, Ground-State Equilibrium Thermodynamics and Switching Kinetics of Bistable [2]Rotaxanes Switched in Solution, Polymer Gels, and Molecular Electronic Devices, *Chem. – Eur. J.*, 2006, **12**, 261–279; (*d*) A. Caballero, F. Zapata and P. D. Beer, Interlocked host molecules for anion recognition and sensing, *Coord. Chem. Rev.*, 2013, **257**, 2434–2455; (*e*) M. J. Langton and P. D. Beer, Rotaxane and Catenane Host Structures for Sensing Charged Guest Species, *Acc. Chem. Res.*, 2014, **47**, 1935–1949.

4 (*a*) C. Kwamen and J. Niemeyer, Functional Rotaxanes in Catalysis, *Chem. – Eur. J.*, 2021, **27**, 175–186; (*b*) S. F. M. van Dongen, S. Cantekin, J. A. A. W. Elemans, A. E. Rowan and R. J. M. Nolte, Functional interlocked systems, *Chem. Soc. Rev.*, 2014, **43**, 99–122; (*c*) V. Blanco, D. A. Leigh and V. Marcos, Artificial switchable catalysts, *Chem. Soc. Rev.*, 2015, **44**, 5341–5370.

5 (*a*) I. Aprahamian, The Future of Molecular Machines, *ACS Cent. Sci.*, 2020, **6**, 347–358; (*b*) L. Zhang, V. Marcos and D. A. Leigh, Molecular machines with bio-inspired mechanisms, *Proc. Natl. Acad. Sci. U. S. A.*, 2018, **115**, 9397–9404; (*c*) S. ErbasCakmak, D. A. Leigh, C. T. McTernan and A. L. Nussbaumer, Artificial Molecular Machines, *Chem. Rev.*, 2015, **115**, 10081–10206; (*d*) C. Cheng and J. F. Stoddart, Wholly Synthetic Molecular Machines, *ChemPhysChem*, 2016, **17**, 1780–1793.

6 N. Pairault, R. Barat, I. Tranoy-Opalinski, B. Renoux, M. Thomas and S. Papot, Rotaxane-based architectures for biological applications, *C. R. Chim*, 2016, **19**, 103–112.

7 J. Riebe and J. Niemeyer, Mechanically Interlocked Molecules for Biomedical Applications, *Eur. J. Org. Chem.*, 2021, 5106–5116.

8 (*a*) C. Wu, P. R. Lecavalier, Y. X. Shen and H. W. Gibson, Synthesis of a rotaxane via the template method, *Chem. Mater.*, 1991, **3**, 569–572; (*b*) G. M. Hübner, J. Gläser, C. Seel and F. Vögtle, High-Yielding Rotaxane Synthesis with an Anion Template, *Angew. Chem., Int. Ed.*, 1999, **38**, 383–386; (*c*) C. Reuter, W. Wienan, G. M. Hübner, J. Gläser, C. Seel and F. Vögtle, High-Yield Synthesis of Ester, Carbonate, and Acetal Rotaxanes by Anion Template Assistance and their Hydrolytic Dethreading, *Chem. – Eur. J.*, 1999, **5**, 2692–2697; (*d*) V. Aucagne, K. D. Hänni, D. A. Leigh, P. J. Lusby and D. B. Walker, Catalytic ''Click'' Rotaxanes: A Substoichiometric Metal-Template Pathway to Mechanically Interlocked Architectures, *J. Am. Chem. Soc.*, 2006, **128**, 2186–2187.

9 (*a*) M. Galli, J. E. M. Lewis and S. M. Goldup, A Stimuli Responsive Rotaxane-Au Catalyst: Regulation of Activity and Diastereoselectivity, *Angew. Chem., Int. Ed.*, 2015, **127**, 13545–13549; (*b*) X.-Q. Wang, W. Wang, W.-J. Li, L.-J. Chen, R. Yao, G.-Q. Yin, Y.-X. Wang, Y. Zhang, J. Huang, H. Tan, Y. Yu, X. Li, L. Xu and H.-B. Yang, Dual stimuli-responsive rotaxane-branched dendrimers with reversible

dimension modulation, *Nat. Commun.*, 2018, **9**, 3190; (*c*) M. Nandi, S. Bej, T. K. Ghosh and P. Ghosh, A multi-functional catenated host for the efficient binding of Eu3+ and Gd3+, *Chem. Commun.*, 2019, **55**, 3085–3088; (*d*) O. Borodin, Y. Shchukin, C. C. Robertson, S. Richter and M. Delius, Self-Assembly of Stimuli-Responsive [2]Rotaxanes by Amidinium Exchange, *J. Am. Chem. Soc.*, 2021, **143**, 16448–16457; (*e*) M. Nandi, S. Bej and P. Ghosh, NDI-integrated rotaxane/catenane and their interactions with anions, *Dalton Trans.*, 2022, **51**, 13507–13514.

10 (*a*) A. Carlone, S. M. Goldup, N. Lebrasseur, D. A. Leigh and A. Wilson, A Three-Compartment Chemically-Driven Molecular Information Ratchet, *J. Am. Chem. Soc.*, 2012, **134**, 8321–8323; (*b*) E. Busseron and F. Coutrot, N-Benzyltriazolium as Both Molecular Station and Barrier in [2]Rotaxane Molecular Machines, *J. Org. Chem.*, 2013, **78**, 4099–4106; (*c*) Y. Matsuoka, Y. Mutoh, I. Azumaya, S. Kikkawa, T. Kasama and S. Saito, Synthesis and Shuttling Behavior of [2]Rotaxanes with a Pyrrole Moiety, *J. Org. Chem.*, 2016, **81**, 3479–3487; (*d*) Y. Mochizuki, K. Ikeyatsu, Y. Mutoh, S. Hosoya and S. Saito, Synthesis of Mechanically Planar Chiral rac-[2]Rotaxanes by Partitioning of an Achiral [2]Rotaxane: Stereoinversion Induced by Shuttling, *Org. Lett.*, 2017, **19**, 4347–4350.

11 (*a*) S. Saito, E. Takahashi and K. Nakazono, Synthesis of [2]Rotaxanes by the Catalytic Reactions of a Macrocyclic Copper Complex, *Org. Lett.*, 2006, **8**, 5133–5136; (*b*) S. Saito, E. Takahashi, K. Wakatsuki, K. Inoue, T. Orikasa, K. Sakai, R. Yamasaki, Y. Mutoh and T. Kasama, Synthesis of Large [2]Rotaxanes. The Relationship between the Size of the Blocking Group and the Stability of the Rotaxane, *J. Org. Chem.*, 2013, **78**, 3553–3560; (*c*) R. Hayashi, Y. Mutoh, T. Kasama and S. Saito, Synthesis of [3]Rotaxanes by the Combination of Copper-Mediated Coupling Reaction and Metal-Template Approach, *J. Org. Chem.*, 2015, **80**, 7536–7546; (*d*) S. Saito, T. Ohkubo, Y. Yamazaki, T. Yokoyama, Y. Mutoh, R. Yamasaki and T. Kasama, A Macrocyclic Phenanthroline–Copper Complex with Less Steric Hindrance: Synthesis, Structure, and Application to the Synthesis of a [2]Rotaxane, *Bull. Chem. Soc. Jpn.*, 2015, **88**, 1323–1330; (*e*) S. Saito, Y. Hirano, Y. Mutoh and T. Kasama, Synthesis of a Homochiral [2]Rotaxane from a BINOL-derived Macrocyclic Phenanthroline, *Chem. Lett.*, 2015, **44**, 1509–1511; (*f*) R. Hayashi, P. Slavík, Y. Mutoh, T. Kasama and S. Saito, Sequence-Selective Synthesis of Rotacatenane Isomers, *J. Org. Chem.*, 2016, **81**, 1175–1184; (*g*) Y. Yamashita, Y. Mutoh, R. Yamasaki, T. Kasama and S. Saito, Synthesis of [3]Rotaxanes that Utilize the Catalytic Activity of a Macrocyclic Phenanthroline–Cu Complex: Remarkable Effect of the Length of the Axle Precursor, *Chem. – Eur. J.*, 2015, **21**, 2139–2145; (*h*) S. Saito, Synthesis of interlocked compounds utilizing the catalytic activity of macrocyclic phenanthroline–Cu complexes, *J. Inclusion Phenom. Macrocyclic Chem.*, 2015, **82**, 437–451.

12 (*a*) D. M. Nguyen, A. Frazer, L. Rodriguez and K. D. Belfield, Selective Fluorescence Sensing of Zinc and Mercury Ions with Hydrophilic 1,2,3-Triazolyl Fluorene Probes, *Chem. Mater.*, 2010, **22**, 3472–3481; (*b*) S. C. Everhart, U. K. Jayasundara, H. J. Kim, R. Procfflpez-Schtirbu, W. A. Stanbery, C. H. Mishler, B. J. Frost, J. I. Cline and T. W. Bell, Synthesis and Photoisomerization of Substituted Dibenzofulvene Molecular Rotors, *Chem. – Eur. J.*, 2016, **22**, 11291–11302; (*c*) Z. Chu, D. Wang, C. Zhang, X. Fan, Y. Tang, L. Chen and D. Zou, Synthesis of Dendritic Oligo-Spiro(fluorene-9,9′-xanthene) Derivatives with Carbazole and Fluorene Pendants and their Thermal, Optical, and Electroluminescent Properties, *Macromol. Rapid Commun.*, 2009, **30**, 1745–1750.

13 A. Sarkar, P. Ilankumaran, P. Kisanga and J. G. Verkade, First Synthesis of a Highly Basic Dendrimer and its Catalytic Application in Organic Methodology, *Adv. Synth. Catal.*, 2004, **346**, 1093–1096.

14 A. Rampa, L. Piazzi, F. Belluti, S. Gobbi, A. Bisi, M. Bartolini, V. Andrisano, V. Cavrini, A. Cavalli, M. Recanatini and P. Valenti, Acetylcholinesterase Inhibitors: SAR and Kinetic Studies on ω-[N-Methyl-N-(3-alkylcarbamoyloxyphenyl)methyl]-aminoalkoxyaryl Derivatives, *J. Med. Chem.*, 2001, **44**, 3810–3820.

15 (*a*) C. Dietrich-Buchecker and J. P. Sauvage, Templated synthesis of interlocked macrocyclic ligands, the catenands. Preparation and characterization of the prototypical bis-30 membered ring system, *Tetrahedron*, 1990, **46**, 503–512; (*b*) S. Saito, K. Nakazono and E. Takahashi, Template synthesis of [2]rotaxanes with large ring components and tris(biphenyl)methyl group as the blocking group. The relationship between the ring size and the stability of the rotaxanes, *J. Org. Chem.*, 2006, **71**, 7477–7480.

16 (*a*) J. D. Megiatto Jr and D. I. Schuster, Alternative Demetalation Method for Cu(I)-Phenanthroline-Based Catenanes and Rotaxanes, *Org. Lett.*, 2011, **13**, 1808–1811; (*b*) K. Ugajin, E. Takahashi, R. Yamasaki, Y. Mutoh, T. Kasama and S. Saito, Synthesis of [2]Rotaxanes by the Copper-Mediated Threading Reactions of Aryl Iodides with Alkynes, *Org. Lett.*, 2013, **15**, 2684–2687.

17 All NMR spectra we discussed in this manuscript were recorded in $CDCl_3$.

18 The assignment is based on the H–F COSY experiment. See ESI† for details.

19 See ESI† (Table S1) for details.

20 A reviewer pointed out that the ring component could be localized in one end of the axle component, and the conformation is stabilized by C–H$\cdots\pi$ interactions. We assume that this is unlikely because in the NMR spectrum of **10Aa** (Fig. 3), for example, the chemical shifts of the protons bound to the dumbbell moiety are similar to those of the axle component **11c**. The chemical shifts of these signals would be affected significantly if the rotaxane adopted the conformation suggested by the reviewer. We thank the reviewer for the valuable suggestions.

21 We assume that the major conformer would be the structure described at the bottom in Fig. 6b, because of the large steric bulk of the TBS group.

22 (*a*) L. D. Movsisyan, M. Franz, F. Hampel, A. L. Thompson, R. R. Tykwinski and H. L. Anderson, Polyyne Rotaxanes: Stabilization by Encapsulation, *J. Am. Chem. Soc.*, 2016, **138**, 1366–1376; (*b*) Y. Kawasaki, S. Rashid, K. Ikeyatsu, Y. Mutoh, Y. Yoshigoe, S. Kikkawa, I. Azumaya, S. Hosoya and S. Saito, Conformational Control of [2]Rotaxane by Hydrogen Bond, *J. Org. Chem.*, 2022, **87**, 5744–5759.